Validation of Global Ozone Monitoring Experiment ozone profiles and evaluation of stratospheric transport in a global chemistry transport model

de Laat, A.T.J.; Landgraf, J.; Aben, I.; Hasekamp, O.; Bregman, B.

published in
Journal of Geophysical Research. Atmospheres
2007

DOI (link to publisher)
10.1029/2005JD006789

document version
Publisher's PDF, also known as Version of record

JOURNAL OF GEOPHYSICAL RESEARCH, VOL. 112, D05301, doi:10.1029/2005JD006789, 2007

Validation of Global Ozone Monitoring Experiment ozone profiles and evaluation of stratospheric transport in a global chemistry transport model

A. T. J. de Laat,[1,2] J. Landgraf,[1] I. Aben,[1] O. Hasekamp,[1] and B. Bregman[3]

Received 20 October 2005; revised 24 August 2006; accepted 5 October 2006; published 2 March 2007.

[1] This paper presents a validation of Global Ozone Monitoring Experiment (GOME) ozone (O_3) profiles which are used to evaluate stratospheric transport in the chemistry transport model (CTM) Tracer Model version 5 (TM5) using a linearized stratospheric O_3 chemistry scheme. A comparison of GOME O_3 profile measurements with independent O_3 sonde measurements at midlatitudes shows an excellent agreement. Differences are smaller than 5%, well within the uncertainty of the O_3 sonde measurements. Within the tropics, the GOME O_3 profile differences are larger, with a clear lower stratospheric negative O_3 bias with compensating positive biases in the troposphere and higher stratosphere. The TM5 model with linearized O_3 chemistry simulates realistic lower and middle stratospheric spatial and temporal O_3 variations on both short (daily) and long (seasonal) timescales. Model stratospheric O_3 is significantly overestimated in the extratropics and slightly underestimated in the tropics, as is also shown in a comparison with Total Ozone Mapping Spectrometer total O_3 column measurements. This model bias predominantly occurs in the lower stratosphere and is present throughout the year, albeit with seasonal variations: The bias is larger during local winter compared with local summer. The particular spatial and seasonal variations of the model bias suggest a too fast meridional stratospheric transport in TM5, which agrees with earlier found shortcomings of using winds from data assimilation systems. The model results are very sensitive to the data assimilation method in the numerical weather prediction that provides the model wind fields. A large reduction (up to 50% of the bias) in modeled lower stratospheric midlatitude O_3 was found when winds from four-dimensional instead of three-dimensional data assimilation were used. Previous work has shown that using different forecast periods was important for improving the age of air. Model results differed with different forecast periods (up to 3 days), although the effect was mainly confined to high-latitude lower stratospheric O_3. Apparently, using different forecast periods is more important for age-of-air calculations than for stratospheric O_3 calculations. A positive bias in the extratropical lower stratosphere of about 20% remained, possibly related to the lack of heterogeneous polar stratospheric O_3 destruction in TM5.

Citation: de Laat, A. T. J., J. Landgraf, I. Aben, O. Hasekamp, and B. Bregman (2007), Validation of Global Ozone Monitoring Experiment ozone profiles and evaluation of stratospheric transport in a global chemistry transport model, *J. Geophys. Res.*, *112*, D05301, doi:10.1029/2005JD006789.

1. Introduction

[2] Recently it was found that stratospheric winds from data assimilation systems (DAS) are inaccurate or contain "noise" as a result of data assimilation in numerical weather prediction (NWP) that provide these winds for most chemistry transport models (CTMs) [*Bregman et al.*, 2006]. Generally, long-lived trace gases like SF_6 and CO_2 are used to study stratospheric transport. Simulation with CTMs indicate that tracers are transported too fast from the tropical to the midlatitude stratosphere [*Waugh and Hall*, 2002; *Douglass et al.*, 2003; *Schoeberl et al.*, 2003; *Meijer et al.*, 2004]. Trajectory experiments showed less dispersion in the lower tropical stratosphere when NWP forecasts were used rather than NWP analyses [*Scheele et al.*, 2005]. By using meteorological forecasts instead of analyses, the model physics would reduce the data assimilation effects and create less "noisy" winds. Using multiday forecasts the winds further improved and the meridional transport in the stratosphere further reduced [*Scheele et al.*, 2005], although

[1] Netherlands Institute for Space Research, Utrecht, Netherlands.
[2] Now at Royal Netherlands Meteorological Institute, De Bilt, Netherlands.
[3] TNO Built Environment and Geosciences, Apeldoorn, Netherlands.

0148-0227/07/2005JD006789$09.00

model diffusion remained an issue [*Meijer et al.*, 2004]. These studies also clearly showed that the largest improvements were achieved when a more sophisticated four-dimensional data assimilation procedure (4DVAR) was used in the NWP, compared to a three-dimensional procedure (3DVAR). So far, these studies focused on trajectories and age-of-air experiments.

[3] *Douglass et al.* [2003] used O_3 measurements to study the representation of stratospheric transport in CTMs and the influence of different meteorological input fields (from data assimilation or climate models), and focused on the tropics with an emphasis on the exchange between tropical troposphere and stratosphere. They found that the CTM data assimilation winds produced unrealistic transport in the lower tropical stratosphere. Using winds from a climate model resulted in a much better CTM performance, and it was concluded that the data assimilation could behave like an additional forcing added to the equations of motion, leading to this fast transport.

[4] Here, we use O_3 measurements to investigate the exchange between the tropical and extratropical stratosphere in the TM5 model. Winds from different data assimilation methods are used which should have different effects on this so-called ''additional forcing'' as noted by *Douglass et al.* [2003], and to test the consistency of their findings compared to this study. We evaluate CTM simulations of stratospheric O_3 with spaceborne O_3 profiles from the Global Ozone Monitoring Experiment (GOME) instrument, O_3 sonde measurements and Total Ozone Mapping Spectrometer (TOMS) total O_3 column measurements. The linearized O_3 chemistry scheme from *Cariolle and Déqué* [1986] was used for the simulation of stratospheric O_3.

[5] The outline of the paper is as follows. Section 2 describes the TM5 model and the linearized O_3 chemistry scheme, the measurements used for this paper (in particular the GOME O_3 profile retrieval method) and presents an extensive validation of the GOME O_3 profile measurements. In section 3, modeled O_3 is evaluated by comparing model results with measurements. Section 4 discusses the sensitivity of the model results to the data assimilation procedure utilized in NWP. The paper ends with a summary and discussion in section 5.

2. Model and Measurements

2.1. TM5 Model

[6] The TM5 model has been developed at the Institute of Marine and Atmospheric research Utrecht (IMAU) in cooperation with the Royal Dutch Meteorological Institute (KNMI) and the Dutch center for Mathematics and Computer Science (CWI). The TM5 model has been used to study stratospheric chemistry and transport [*Bregman et al.*, 2003; *van den Broek et al.*, 2003, 2004]. A detailed description of the TM5 model is given in work by *Krol et al.* [2005]. TM5 uses meteorological information from the European Centre for Medium-Range Weather Forecasts (ECMWF), which has recently been extended vertically to 0.1 hPa. An important improvement in our preprocessing of the ECMWF winds is a new mass conservative transformation of the spectral data to gridded mass fluxes [*Segers et al.*, 2002, 2005]. This new preprocessing ensures mass conserving 3D mass fluxes by calculating physically consistent vertical mass fluxes for every vertical layer separately. Mass imbalance is a general problem in most CTMs [e.g., *Joeckel et al.*, 2001]. The new preprocessing algorithm significantly improves the vertical transport in the tropopause region [*Bregman et al.*, 2003; *Segers et al.*, 2005]. Dispersion of tracers is described by the widely used non-diffusive second moments advection scheme.

[7] For the current model study the horizontal resolution is $3^\circ \times 2^\circ$ (longitude-latitude). All ECMWF levels between 75 and 300 hPa are used while, outside this range, only every second level is used (similar to those of *van den Broek et al.* [2003]). The top model level is located at 0.1 hPa ($\sim$60 km). We use different ECWMF meteorological data sets. We explore the ECMWF reanalyses (ERA40) on the basis of 3DVAR data assimilation and the ECWMF operational data (OD) on the basis of the more sophisticated 4DVAR data assimilation. All meteorological data have a time resolution of 6 hours. In addition, we investigate the impact of the forecast length by using 1-, 2- and 3-day forecasts. TM5 simulations were done for different period because of differences in availability of ERA40 and OD output. For comparison of TM5 with GOME measurements stratospheric O_3 is simulated using ERA40 data for the period January 1996 to December 1998 because of the degradation of the GOME instrument from the beginning of 1999 onward which affects the O_3 profile retrievals [*Dobber et al.*, 1998; *van der A et al.*, 2002]. For comparison of the different assimilation schemes the period January 2000 to December 2001 was simulated: OD output is only available from October 1999 onward while the ERA40 reanalysis is only available up to August 2002. TM5 model simulations with different forecast periods (24, 48 and 72 hours) could only be done for June 2002 to May 2003. Therefore, and because of the GOME degradation, no TM5 simulations with OD can be compared with GOME measurements.

2.2. Linearized O_3

[8] The O_3 chemistry scheme used for this model simulation is the linearized O_3 chemistry described by *Cariolle and Déqué* [1986] and *McLinden et al.* [2000]. It describes stratospheric O_3 variations on the basis of temperature, the thickness of the O_3 layer above a certain model grid and O_3 itself:

$$\frac{dO_3}{dt} = (P - L)[O_3, T, cO_3] \tag{1}$$

[9] The O_3 tendency equals the production and loss of O_3 ($P - L$) which itself is a function of the temperature, O_3 itself and the O_3 column above the grid point under consideration (cO_3). Equation (1) can be expanded as a first-order Taylor series:

$$\frac{d\mathbf{O}_3}{dt} = (P - L) + \frac{\partial(P - L)}{\partial O_3}(\mathbf{O}_3 - O_3) + \frac{\partial(P - L)}{\partial T}(\mathbf{T} - T) + \frac{\partial(P - L)}{\partial cO_3}(\mathbf{cO}_3 - cO_3) \tag{2}$$

where the terms in bold are the actual model fields (O_3 and cO_3 from the CTM and T from the assimilation data). The other terms are climatological values, which are taken from

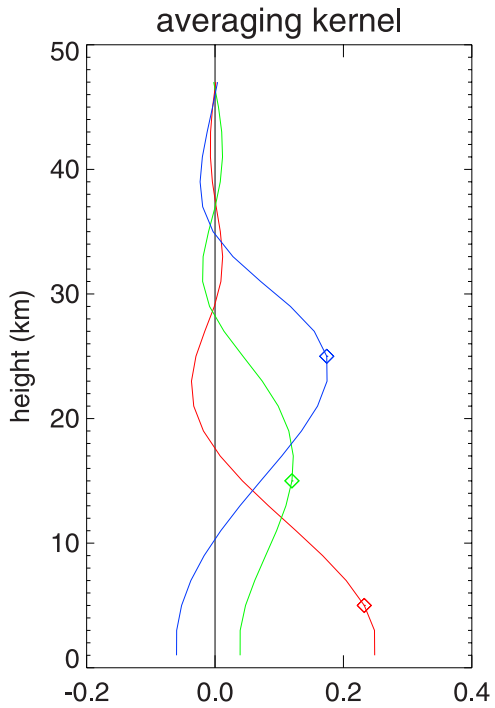

Figure 1. Averaging kernels corresponding to 5, 15, and 25 km as determined from a GOME O_3 profile retrieval for Payerne, Switzerland, 23 June 1996. The markers indicate the altitude for which the averaging kernel is representative.

a two-dimensional full stratospheric chemistry model simulation [*Cariolle and Déqué*, 1986]. The advantage of this scheme is that it is computationally very efficient, and can be readily incorporated in CTMs to test the model performance whereas more complex chemical schemes quickly become computationally expensive. The disadvantage is that this scheme may not accurately describe O_3 variability where O_3 chemistry is more important than transport [*McCormack et al.*, 2004], like the lower and middle troposphere, the upper stratosphere and under conditions of polar O_3 loss chemistry [*Brasseur et al.*, 1999]. On the other hand, in other regions where transport dominates O_3 variability the linearized O_3 chemistry provides a good representation of the actual O_3 tendencies [*McLinden et al.*, 2000]. Its usefulness has been demonstrated in many other studies [e.g., *McLinden et al.*, 2000; *Bregman et al.*, 2001; *Olsen et al.*, 2004], including modeling studies on middle latitude stratospheric O_3 variability and dynamics [*Braesicke and Pyle*, 2003; *Hadjinicolaou and Pyle*, 2004; *Hadjinicolaou et al.*, 2005].

2.3. Measurements

[10] For this study three different sources of (stratospheric) O_3 measurements have been used: O_3 sonde measurements, TOMS total O_3 column measurements and GOME O_3 profile measurements. The O_3 sonde measurements provide detailed vertical information but have limited spatial and temporal coverage. For most stations used here, typically only two O_3 sonde measurements per month were available, with the exception of Hohenpeissenberg and Payerne (one or more per week). The GOME O_3 profile measurements have a better spatial and temporal coverage (typically one profile every 3 days) but less vertical information. The GOME O_3 profile measurements are also less reliable at high latitudes and to a lesser extent in the tropics for reasons provided later in this section. TOMS total O_3 columns have an excellent spatial and temporal coverage, but do not provide any vertical information. Each of these three independent O_3 measurements provides information on different spatial and temporal scales and nicely complement each other to represent the complete range of stratospheric O_3 variability.

[11] Sonde observations are used to assess the GOME O_3 vertical profiles. The O_3 sonde measurements are obtained from the World Ozone and Ultraviolet Data Center (WOUDC; http://www.woudc.org). Total O_3 column measurements are from the Total Ozone Mapping Spectrometer, version 7 [*McPeters et al.*, 1996]. The O_3 sonde and TOMS total O_3 column data sets are widely used for many different applications and require no additional description.

[12] Vertical O_3 profiles are retrieved from GOME spectral measurements with a method that is described in more detail by *Hasekamp and Landgraf* [2001], *Hasekamp et al.* [2002], and *Landgraf and Hasekamp* [2002]. The vertical information content of O_3 that can be obtained from the GOME spectral measurements is limited, typically about five independent pieces of information [*Liu et al.*, 2005]. As a result, the retrieved O_3 profile x is a smoothed form of the true O_3 profile x_{true}, i.e., without fine-scale structures. The relationship between the retrieved and the true profile is given by

$$x = Ax_{true} + e_x$$

where A is the averaging kernel and e_x is the error on the profile resulting from the measurement error [*Rodgers*, 1990]. The GOME O_3 concentrations at a given altitude represents a smoothed average over a certain altitude range rather than the O_3 concentration at this altitude (see Figure 1), although this altitude generally corresponds to the maximum in the averaging kernel. For comparing GOME with measured and modeled O_3 profiles the averaging kernel must be applied to the measured or modeled O_3 profiles. The GOME O_3 profile extends up to 50 km whereas the sonde measurements do not exceed the 30–35 km. Therefore O_3 sonde observations have been extended above 30–35 km with an O_3 climatology [*Fortuin and Kelder*, 1998]. Without this extension it is not possible to apply the averaging kernel to the sonde O_3 profiles. The smoothing of the O_3 sonde profiles in combination with the use of an O_3 climatology above 30–35 km results in a transition zone between the sonde observations and the climatology around 30–35 km. Consequently, the "smoothed" sonde profile above approximately 30 km does not represent independent measurements anymore because of the averaging kernel. However, the main focus of this paper is on lower stratospheric O_3 variability (see section 2.1), where we find most of the O_3 and the largest stratospheric variability and where the parameterized ozone chemistry is most reliable.

[13] It should be noted that because of the averaging kernel negative concentrations can occur in a smoothed O_3 profile. For example, the red curve in Figure 1, representing the 5 km row vector of the averaging kernel, is negative

Table 1. O_3 Sonde Stations Used for Validation of the GOME O_3 Profile Measurements[a]

Station	Station Number	Location		GOME Number	Sonde Number
		Longitude	Latitude		
Sondankyla	1	26.51°E	67.34°N	177	6
Lerwick	2	1.18°E	60.13°N	89	9
Churchill	3	94.07°W	58.75°N	286	26
Edmonton	4	114.10°W	53.55°N	439	55
Goose Bay	5	60.36°W	53.5°N	316	37
Legionowo	6	20.97°W	52.4°N	491	64
Lindenberg	7	14.12°E	52.21°N	461	58
De Bilt	8	5.19°E	52.10°N	493	64
Praha	9	14.45°E	50.02°N	498	61
Hohenpeissenberg	10	11.02°E	47.08°N	477	154
Payerne	11	6.57°E	46.49°N	432	197
Sapporo	12	141.32°E	43.06°N	426	40
Wallops Island	13	75.48°W	37.93°N	398	57
Tateno	14	140.10°E	36.06°N	411	58
Kagoshima	15	130.57°E	31.58°N	371	35
Naha	16	127.68°E	26.2°N	305	28
Nairobi	17	36.8°E	1.27°S	298	17
Ascension	18	14.42°W	7.89°S	299	26
Samoa	19	170.56°W	14.25°S	243	29
Laverton	20	144.75°E	37.87°S	265	28
Macquarie Island	21	158.97°E	54.5°S	409	17

[a]The stations are listed according to latitude. Indicated in the last two columns are the number of GOME and sonde O_3 profile measurements that were available for the period April 1996 to December 1998. The O_3 sonde measurements are obtained from the World Ozone and Ultraviolet Radiation Data Centre (WOUDC; http://www.woudc.org).

between 18 and 29 km. For a troposphere with low O_3 concentrations the negative contribution by the averaging kernel above 18 km can offset the positive contribution of O_3 below 18 km. This effect mainly occurs within the tropics, where O_3 concentrations can become low throughout the tropical troposphere.

2.4. Validation of GOME O_3 Profiles

[14] Sonde measurements were used for the period January 1996 to December 1998 to assess the O_3 GOME profiles (locations listed in Table 1 and shown in Figure 2). At low solar zenith angles, the retrieved GOME O_3 profiles become less sensitive to the lower atmosphere because of longer photon path lengths. For the retrieval algorithm used in this study, this effectively restricts the latitude range of usable O_3 profiles from roughly 60°N to 60°S.

[15] Figure 3 shows the mean of all GOME O_3 profiles collocated with O_3 sonde measurements a Northern Hemisphere, tropical and Southern Hemisphere locations as well as TM5 model results (see section 3). The averaging kernel

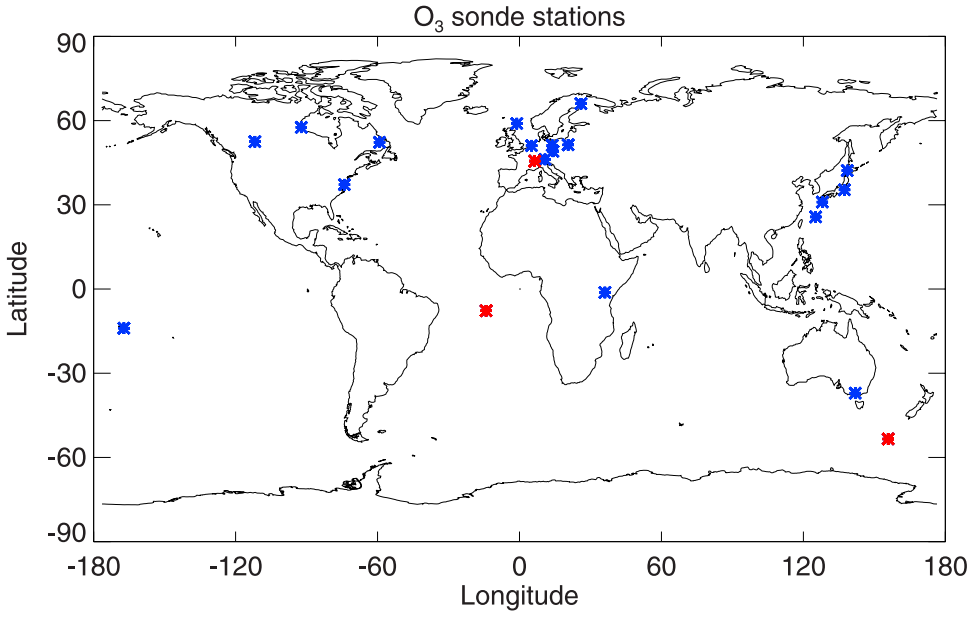

Figure 2. Geographical location of the O_3 sonde stations as presented in Table 1. The red markers indicate the locations in Figure 3.

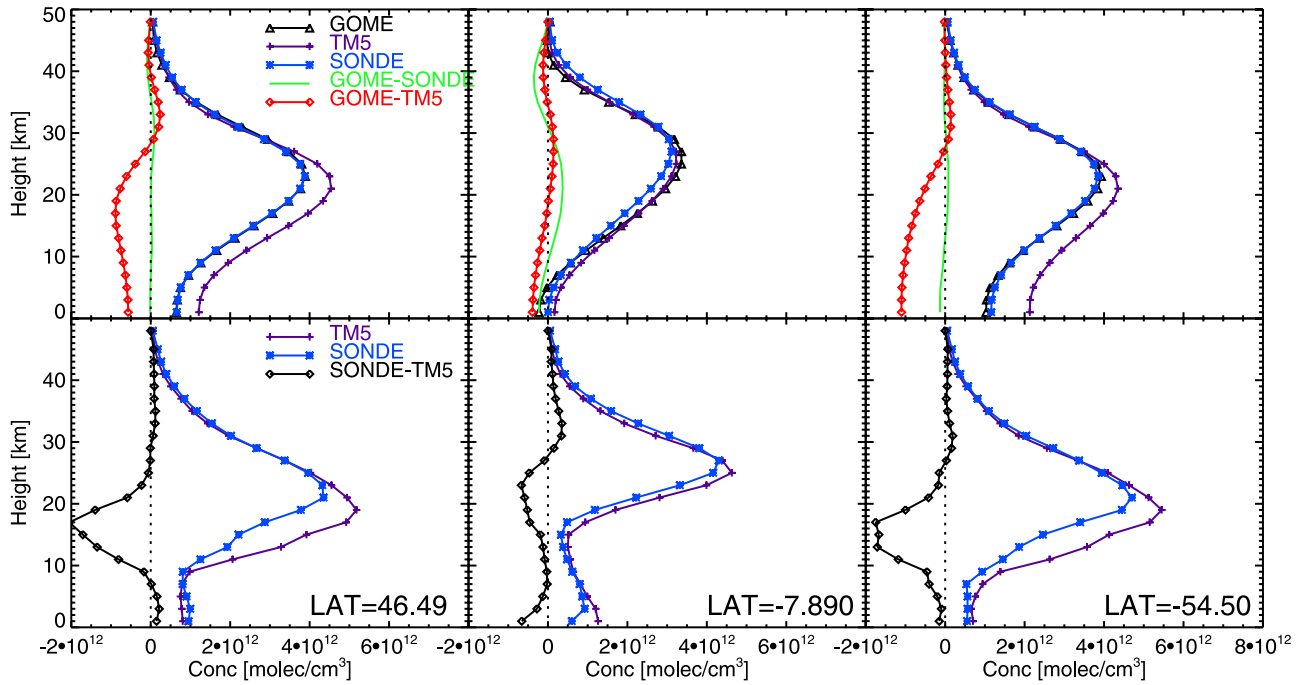

Figure 3. Comparison between measured (GOME, sondes) and modeled (TM5) average O_3 profiles for three different locations for the period January 1996 to December 1998: Payerne (latitude 46.49°), Ascension (latitude −7.89°), and Macquarie Island (latitude −54.5°). (top) Mean O_3 concentration profile for GOME (black), TM5 (purple), and O_3 sonde (blue) as well as the differences between GOME and TM5 (red) and GOME and the O_3 sondes (green). The GOME averaging kernel has been applied to both modeled and sonde-measured O_3 profiles, and only sonde measurements which coincide with GOME O_3 profile measurements are used. (bottom) Same as the top plots but for sonde and TM5 profiles without applying the averaging kernel.

has been applied to the sonde and TM5 O_3 profiles. Note that the sonde measurements have associated errors of up to 5% [*Harris et al.*, 1998]. According to Figure 3, a good agreement exists between average GOME and sonde O_3 profiles for Payerne and Macquarie Island: differences are smaller than 0.1×10^{12} molecules/cm^3 (<2% below 30 km). Above approximately 30 km, the relative differences become larger because of the climatology that has been used to extend the sonde profiles beyond 30–35 km. For the tropical location (Ascension) differences are larger although still smaller than 0.5×10^{12} molecules/cm^3, and the GOME profiles clearly capture the high-altitude O_3 maximum in the tropics. This positive bias between 10 and 30 km is offset by negative biases below 10 km and above 30 km, as evidenced by the fact that the total columns amounts from sonde, GOME profiles and TOMS total O_3 column measurements agree within 2%. These differences in the tropics will be discussed later on.

[16] Figure 4 shows the differences between GOME and the sonde measurements after applying the averaging kernel to the sonde measurements for individual stations at both 15 and 25 km. GOME and sonde measurements agree very well outside of the tropics. Within the tropics, the GOME observations overestimate stratospheric O_3 by up to 30%. As was noted before it appears that this discrepancy is a retrieval artifact. The tropical O_3 profile has relatively low O_3 concentrations in the troposphere and a sharp gradient around the tropopause. The GOME spectral measurements have a coarse vertical resolution, reflected by the broad averaging kernels (see, for example, Figure 1). Negative side lobes of the averaging kernel can lead to negative concentrations in case of a tropical O_3 profile when a negative side lobe occurs at the stratospheric O_3 maximum. Unphysical negative solution elements obtained during the iterative retrieval process are reset to positive values. This affects the retrieved O_3 profiles apparently in such a way that a positive bias occurs in the retrieved stratospheric O_3 profile between 10 and 30 km which is compensated by a negative bias below 10 km and above 30 km (see Figure 3).

[17] Time correlations between GOME and sonde measurements are calculated to evaluate modeled O_3 temporal variability. The correlation calculations use all available sonde and corresponding GOME measurements. Figure 5 shows the correlation between the GOME-measured O_3 concentrations (dark gray bars) and the individual sonde stations for the same altitudes as in Figure 4. Sonde-GOME correlations are high in the extratropics exceeding 0.9. Within the tropics, the correlations between TM5 and GOME are significantly lower than between sondes and GOME, especially at 25 km. Time variability of tropical upper tropospheric and stratospheric O_3 is also considerably smaller than at midlatitudes; hence correlations are lower as temporal variations due to measurement noise become more important relative to the actual tropical stratospheric O_3 variations.

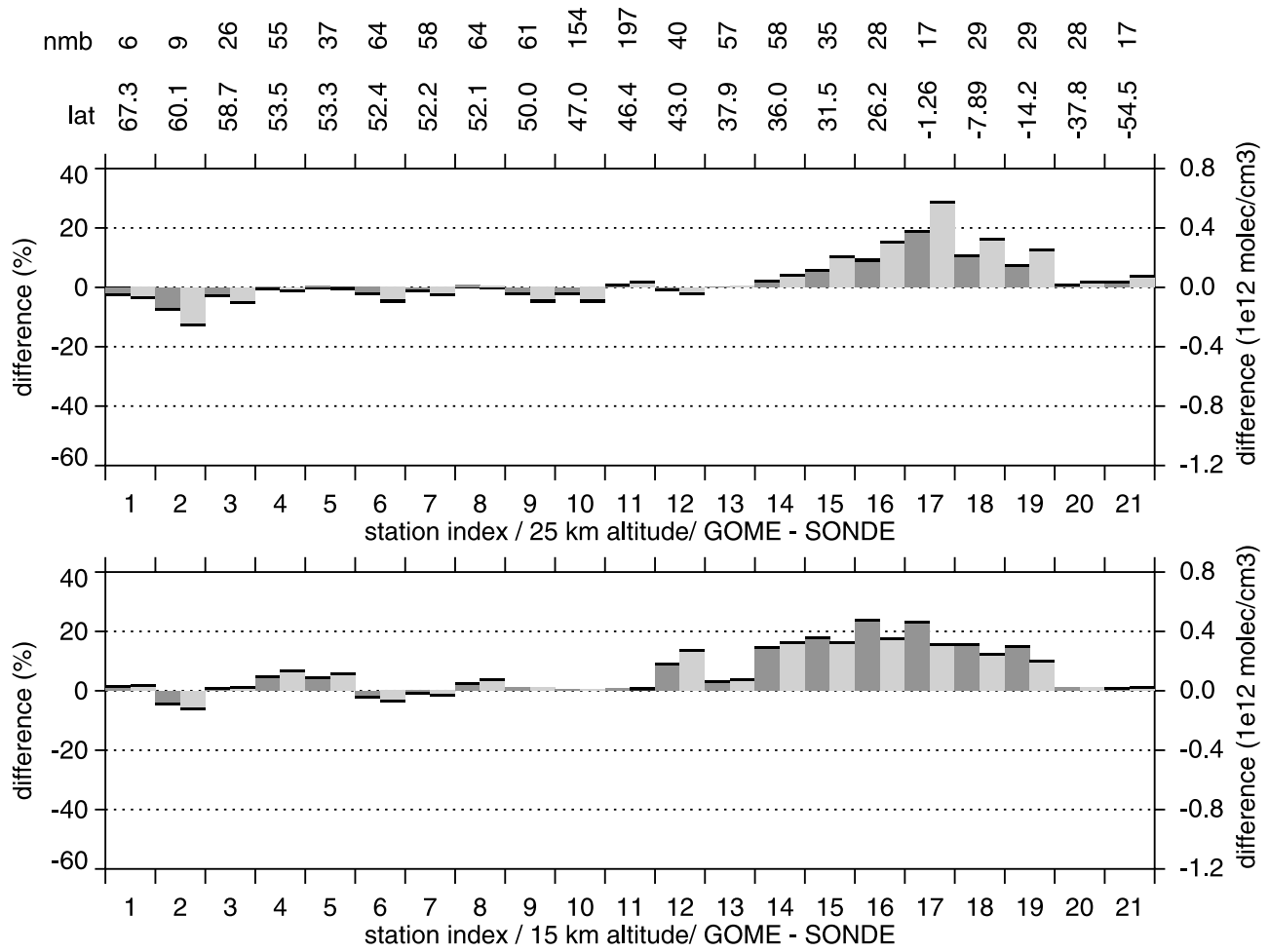

Figure 4. Average differences between GOME and sonde measurements for all sonde locations (Table 1) for all available sonde measurements for the period January 1996 to December 1998 at 15 and 25 km. The top plot shows the differences at 25 km, and the bottom plot shows the differences at 15 km. The light bars are the absolute differences (molecules/cm^3), and the dark bars indicate the relative differences (%). Stations are sorted according to latitude (north to south is from left to right) and are numbered according to the second column in Table 1. Indicated above the figure are the latitude of the stations and the number of measurements that have been used for each individual station (see also Table 1). For the sonde measurements, the GOME averaging kernel has been applied, and only sonde measurements which coincide with GOME O_3 profile measurements are used.

[18] Root-mean-square (RMS) differences between GOME and sonde measurements vary between 2 and 5 10^{11} molecules/cm^2 in the troposphere and stratosphere up to 30 km. In the stratosphere this translates into differences smaller than 10%; in the troposphere differences are larger (typically 30–40%) because of the larger tropospheric O_3 variability and smaller total O_3 amounts. Differences are also relatively large above 30 km because of the climatology that dominates the sonde measurements above 30 km. The RMS differences are comparable to validation results of other retrieval algorithms [*Hoogen et al.*, 1999; *Liu et al.*, 2005], although comparison of validation results is complicated because of the use of a priori information in the other retrieval algorithms. The GOME O_3 profile retrieval used for this study do not use a priori data and only smooth O_3 profiles can be retrieved, directly reflecting the information content of the spectral measurements. Other methods generally use a priori information and therefore have more small-scale profile structures.

[19] Summarizing, we conclude that the GOME O_3 profiles agree well with the measured sonde profiles in the extratropics and can be used for evaluating the TM5 simulations in those regions. The GOME O_3 profiles are less accurate within the tropics as a bias has been identified that likely is related to the retrieval method, but which does not have a large effect on the total O_3 column values on the basis of the GOME O_3 profiles.

3. Comparison of O_3 Measurements With TM5

3.1. Averages

[20] As evident in Figure 3, the differences between GOME and the TM5 modeled O_3 profiles are significantly larger than the differences between GOME and sonde O_3 profiles. The TM5 simulation was done using ERA40

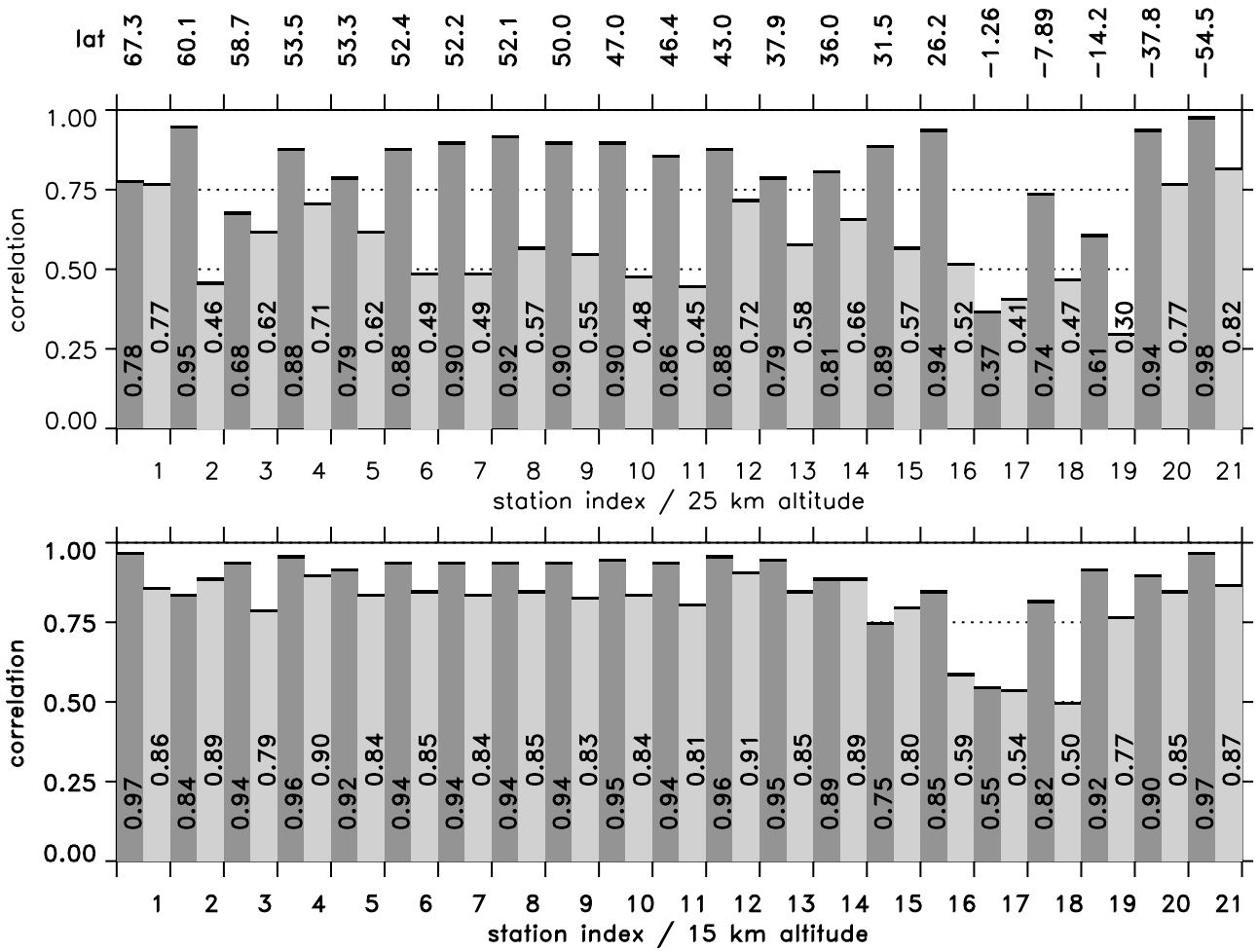

Figure 5. Correlation coefficients between the GOME measured O_3 profiles and sonde and TM5 modeled O_3 concentrations for the same measurements used in Figure 4. The dark bars indicate the GOME-sonde time correlation, and the light bars indicate the GOME-TM5 time correlation.

reanalysis output. The model overestimates O_3 concentrations below 25 km at midlatitudes. Above 25 km the average measured and modeled concentrations are comparable. A direct comparison between sonde observations and model results (bottom plots in Figure 3), i.e., without applying the averaging kernel, shows that the differences are confined to the layer between 10 and 25 km, i.e, the middle to lower stratosphere and tropopause region. Furthermore, this bias is absent in the tropics. Measured and modeled average tropospheric O_3 agree quite well. However, we are cautious drawing too much attention to this region for which the linearized O_3 chemistry scheme is not ideally suited (see also section 3.2).

[21] Figure 6 shows the average differences between the sonde and TM5 O_3 concentrations for the period January 1996 to December 1998 at two stratospheric altitudes (15 and 25 km) without applying the averaging kernels for different stations. The stratospheric model O_3 bias at 15 km as seen in Figure 3 is consistently found for all midlatitude stations: modeled O_3 is about 40–50% or $1-2 \times 10^{12}$ molecules cm^{-3} too high. For the three tropical stations (17–19), the differences are smaller at only about 2×10^{11} molecules cm^{-3}. This lower value may be due to the fact that 15 km in the tropics is still tropospheric but may also reflect the shortcoming of using parameterized O_3 chemistry in the troposphere.

[22] At 25 km modeled and measured extratropical concentrations are comparable, with the exception of the two most northern stations where a large positive model bias is found. These stations have a poor measurement frequency with less than 10 measurements over the period under consideration and therefore cannot be considered representative for an annual mean. Tropical stations show a small positive model bias for Ascension and Nairobi, although not for Samoa. The tropical model biases vary with season, although sonde measurements used for Figures 3 and 6 for Ascension and Nairobi are not equally distributed over the seasons, introducing an additional sampling bias. However, the tropical model biases are small (10% or less) compared to the large midlatitude lower stratospheric model bias at 15 km.

3.2. Individual Stations: Variability

[23] In section 3.1, the average measured and modeled O_3 concentrations at different altitudes were compared. However, the comparison of mean concentrations does not reveal whether the model reproduces measured temporal variabil-

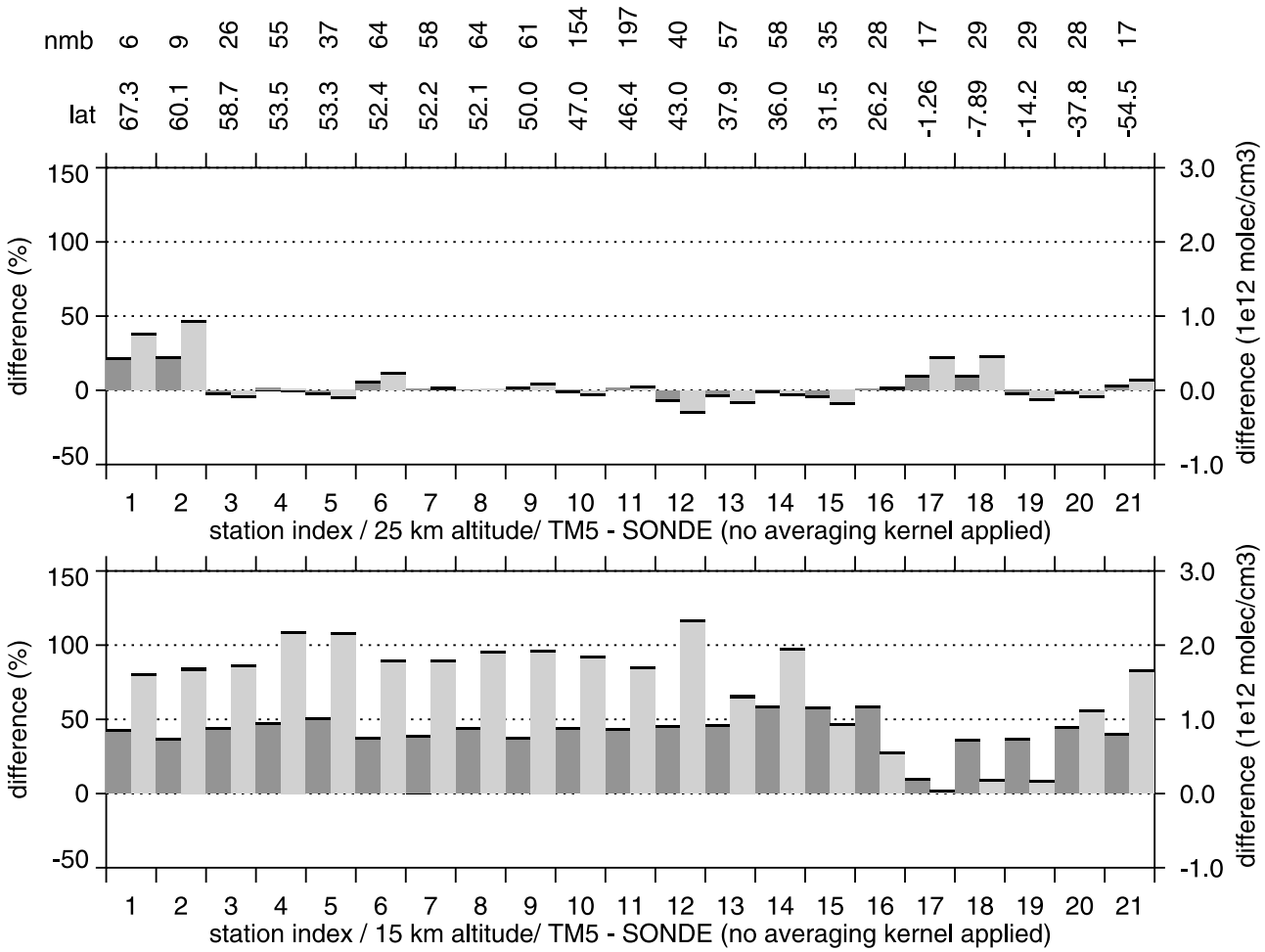

Figure 6. As in Figure 4 but for the TM5-sonde differences but without applying the averaging kernel.

ity. An example of the modeled versus measured O_3 concentrations is given in Figure 7 which shows the O_3 concentrations at 15 km for Payerne, Switzerland, after applying the averaging kernel. Modeled O_3 concentrations have been adjusted such that the average modeled O_3 concentration equals the average measured concentration (the model bias in Figure 3). A good correlation exists between measured and modeled O_3 concentrations. The model reproduces both measured seasonal and shorter-time O_3 variations. The wintertime lower stratospheric O_3 concentrations are varying at synoptic timescales (days–weeks) related to Rossby waves, baroclinic instability and associated frontal activity. During summer, when frontal activity is less pronounced, the O_3 variations are also smaller in the tropopause region.

[24] Figure 5 also shows the correlation between the GOME-measured O_3 concentrations and TM5 results. Correlations at 15 km are high outside of the tropics and lower within the tropics, similar to the sonde-GOME comparison, and related to the much smaller variability in tropical stratospheric O_3. The correlations for the GOME-TM5 comparison are in general slightly lower than for the GOME-sonde comparison. At 25 km correlations between GOME and TM5 results are significantly lower than between GOME and sonde measurements. Because of the smoothing of averaging kernel the 25 km GOME measurement is also affected by upper stratospheric O_3 for which the linearized O_3 chemistry scheme is less well suited as explained in section 2.3, leading to lower correlations at higher altitudes for GOME and TM5 compared to GOME and sondes.

3.3. Zonal Stratospheric O_3 Variability

[25] The comparison of TM5 with O_3 sonde measurements shows an overestimation by the model in the lower stratosphere in the extratropics. However, the latitudinal extent of this overestimation is difficult to determine since the sonde measurements have limited latitudinal coverage. Zonal stratospheric O_3 variations are much smaller than meridional variations and one particular longitude represents typical meridional stratospheric O_3 variations. Therefore GOME O_3 profiles were retrieved along a latitudinal cross section over the central Pacific (170°W) and were compared with the model results to investigate the latitudinal extent of the model biases in more detail. One longitude over 1 year (April 1996 to March 1997) was selected because the GOME O_3 profile retrieval algorithm is computationally expensive. Figure 8 shows the mean O_3 concentration, covering one complete year of measurements, along 170°W for both TM5 and GOME as a function of latitude and height as well as their differences. The top two plots of Figure 8 show that the TM5 model reproduces the

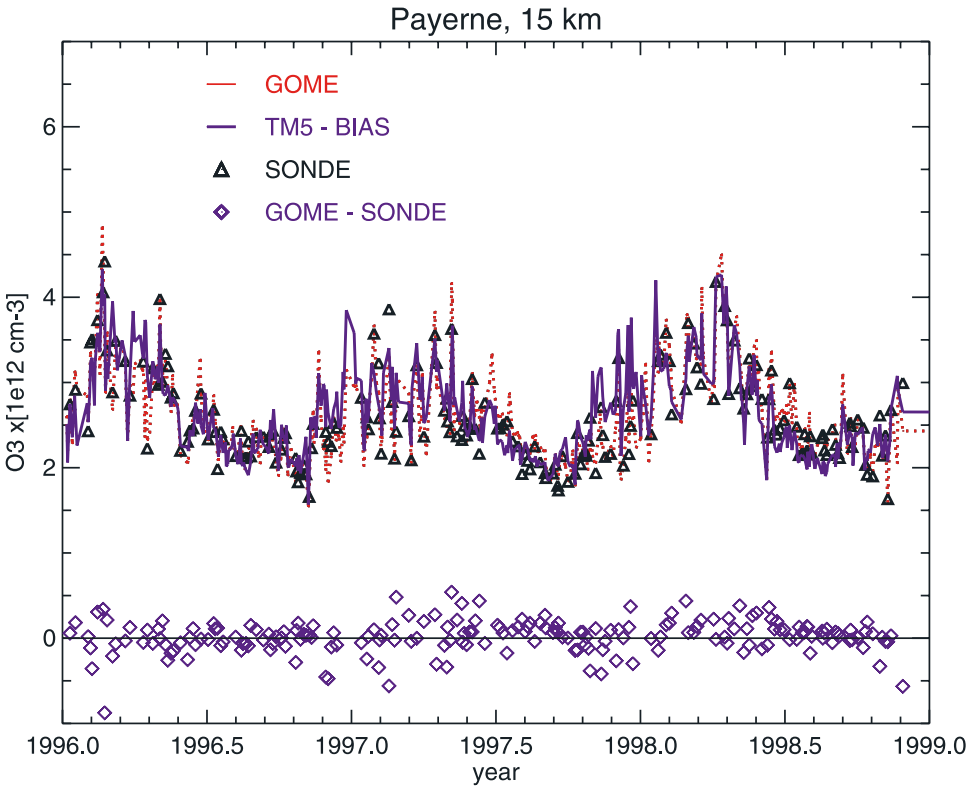

Figure 7. O_3 concentration at 15 km for Payerne for GOME (red), TM5 model (purple), and O_3 sondes (black). The model concentrations have been adjusted so that the mean modeled (TM5) and measured (GOME) concentrations are similar. Indicated also are the differences between GOME and O_3 sonde concentrations (purple diamonds).

large-scale O_3 variations in both the troposphere and stratosphere as measured by GOME. The bottom plot Figure 8 shows the differences between GOME and TM5. In the tropical stratosphere up to 30 km, modeled O_3 concentrations are lower than measured by GOME. As outlined earlier and shown in Figure 4, the retrieved GOME profiles in the tropics contain positive measurement biases which partially explain the tropical stratospheric model bias. However, it cannot fully explain the differences, hence a part of the negative tropical stratospheric model bias is likely real.

[26] In the tropical troposphere and throughout the lower atmosphere at high latitudes, modeled O_3 concentrations are too high. Differences in the Northern Hemisphere are largest in the lower stratosphere and upper troposphere whereas, for the tropics and the Southern Hemisphere, differences are largest closer to the surface. Note that a clear separation between troposphere and stratosphere cannot be made because of the averaging kernels.

[27] Figure 8 clearly shows a hemispheric extent of the model overestimation in the lower stratosphere, suggesting a large-scale bias in the meridional transport (Brewer-Dobson circulation [*Brewer*, 1949; *Dobson*, 1956]). This circulation is directed from the tropics to midlatitudes [*Dessler*, 2000]. The tropical stratosphere is an O_3 source region whereas the midlatitude stratosphere is an O_3 destruction region. The Brewer-Dobson circulation thus causes a net transport of O_3 from the tropical to the midlatitude stratosphere. If this transport is too fast in the model, too much stratospheric O_3 is transported from the tropical source region. This O_3 accumulates in the extratropical lower stratosphere and too little O_3 remains in the tropical stratosphere. Most of the tropical deficit is balanced by increased O_3 production due to the reduced tropical total O_3 column. Furthermore, the meridional stratospheric circulation has its maximum strength during local winter and is stronger in the Northern Hemisphere than in the Southern Hemisphere. The effect of the too fast transport is thus largest in the Northern Hemispheric winter. However, interpretation of differences between GOME and TM5 is hampered by the averaging kernel. Figure 3 clearly shows that because of the smoothing O_3 below 10 km is partly "stratospheric." The Southern Hemispheric midlatitude differences in the bottom plot of Figure 8 are likely related to the TM5 stratospheric bias as the tropospheric bias is relatively small (see Figure 3).

3.4. Statistics and Probability Distribution Functions

[28] One of the advantages of using satellite data is the large amount of available measurements. For example, there were more than 250 collocations with GOME at nearly all sonde station locations. At most midlatitudes, the number of collocations even exceeded 400 (about one measurement every 3 days). In order to yield a more quantitative and clearer view of the model bias at certain altitudes, we further evaluate the model results by using probability distribution function (PDF). Each PDF presented here is a distribution of the probability of occurrence of a measured or modeled

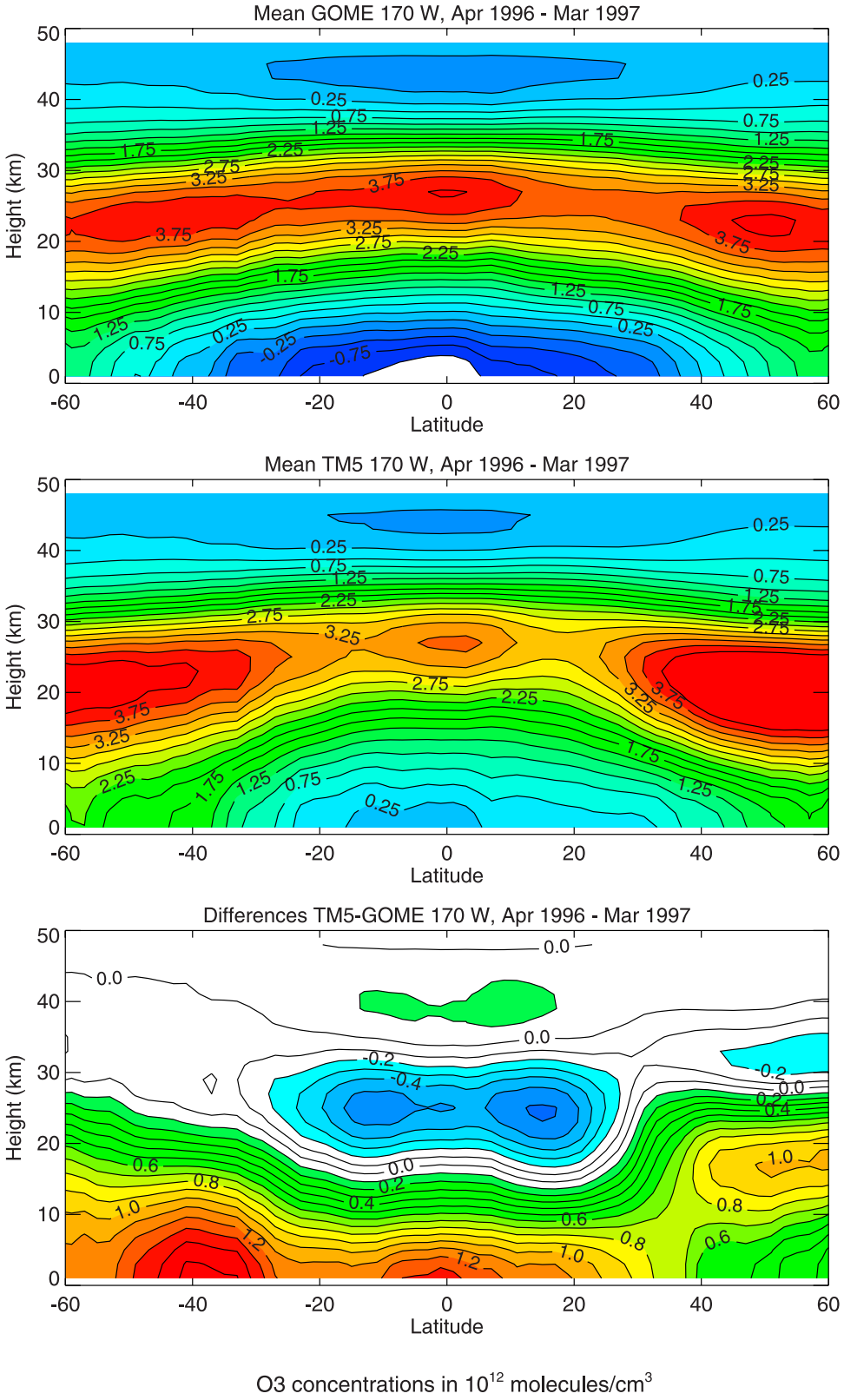

Figure 8. Vertical distribution of TM5 and GOME O_3 along 170°W from 60°N to 60°S for April 1996 to March 1997. (top) Mean O_3 concentrations for GOME. (middle) Mean O_3 concentrations for TM5 after applying the averaging kernel. (bottom) Differences between TM5 and GOME O_3 concentrations. O_3 concentrations are in molecules/cm^2.

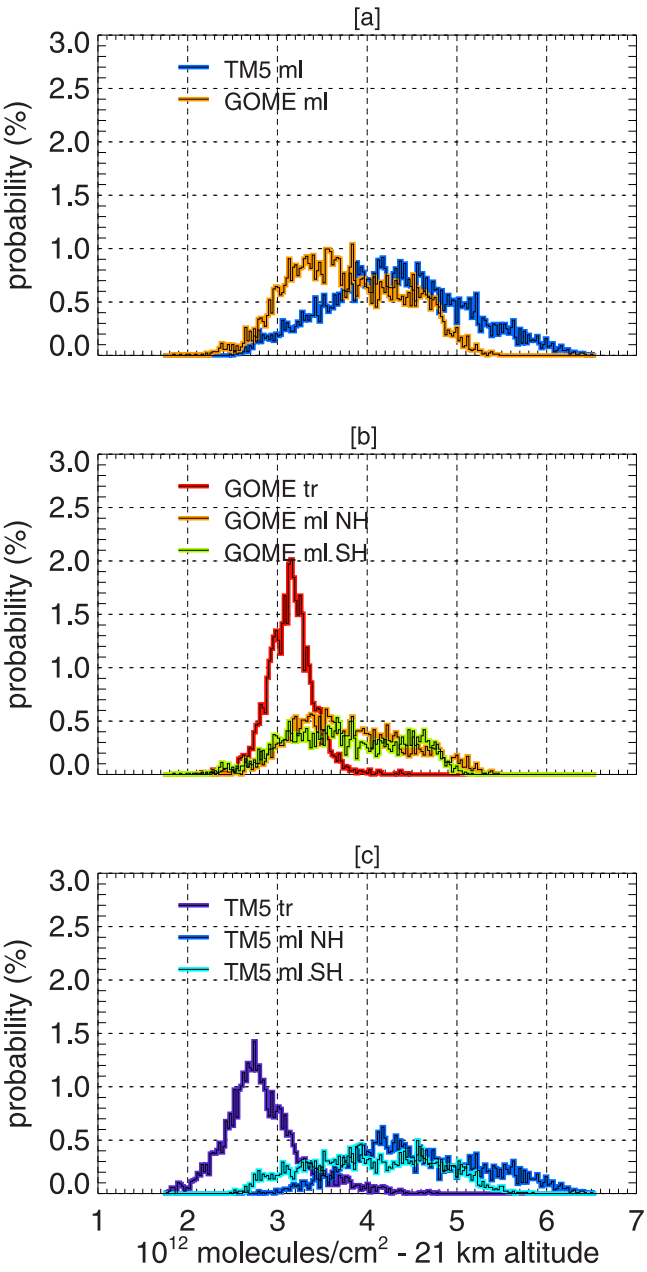

Figure 9. Probability density distribution (PDD) of GOME and TM5 O_3 concentrations for the same data as used for Figure 8 for the altitude of 21 km. Probability is given as percentage of the total number of data points. (a) GOME (orange) and TM5 (blue) for middle latitudes (60°N–30°N and 30°S–60°S). (b) GOME for Northern and Southern hemisphere midlatitudes and tropics. (c) TM5 for Northern and Southern hemisphere midlatitudes and tropics.

O_3 concentration at a given altitude within a certain O_3 concentration interval. This method has been used for other satellite measurements [*Rood et al.*, 2000; *Strahan and Douglass*, 2004]. PDFs have been compared for the tropics, northern and Southern Hemisphere midlatitudes at 21 km altitude.

[29] Consistent with the previous findings, the measured midlatitude PDFs are similar (Figure 9a), but the modeled concentrations are systematically too high. The measurement PDF is slightly narrower than the model PDF. Figures 9b and 9c show the GOME measurement and TM5 model PDFs for the midlatitudes in both hemispheres. The measurement PDFs have a very similar width and amplitudes for both hemispheres. This is not the case for the model PDFs. Rather, model PDFs are broader than measurement PDFs with on average more O_3 in the Northern Hemisphere. As noted in section 3.3. the largest effect of a too strong meridional stratospheric circulation (too high O_3) will thus occur in the Northern Hemisphere. During local summer transport is weak but O_3 continues to be destroyed in the midlatitude stratosphere. Destruction of O_3 is larger for higher O_3 concentrations so that at the end of local summer the stratospheric O_3 excess will be lower (see also section 3.5).

3.5. Comparison of TM5 Total O_3 Columns With TOMS Measurements

[30] The previous sections have shown that biases exist in the model results, which have a clear meridional signature. A comparison was made between modeled and measured total O_3 columns to investigate the zonal structure and seasonal variations of the biases in more detail. Figure 10 shows the zonal monthly mean total O_3 columns from TM5 and TOMS for the period January 1996 to December 1998. It should be noted that for 1996 TOMS measurements are only available from August onward. The seasonal cycle and the zonal variations as observed in the TOMS measurements are reproduced by TM5. Modeled tropical total O_3 columns are slightly smaller than measured. Modeled midlatitude total O_3 columns are significantly larger than measured. The largest differences are found over polar regions and vary with season: the largest differences occur during local winter while the smallest appear during local summer. The differences occur systematically throughout the year poleward of 30°. Heterogeneous polar O_3 loss occurs only poleward of 60° and only during late winter and early spring [*Hadjinicolaou and Pyle*, 2004], and thus cannot account for a large part of the differences between TM5 and TOMS. Furthermore, an incorrect representation of tropospheric O_3 in the model, especially in the Southern Hemisphere (see, for example, Figure 8), might also cause some differences but cannot explain differences of 50 DU or more on a global scale at midlatitudes.

[31] The seasonal variation and spatial extent of the total O_3 column differences are consistent with the findings from previous sections, namely that the strongest effect of the too fast meridional stratospheric circulation occurs at Northern Hemisphere midlatitudes during local winter. During local summer, transport of O_3 from the source region is reduced while O_3 destruction continues, thus reducing the model bias during local summer at midlatitudes.

4. TM5 Model Sensitivity to Meteorological Assimilation Procedure and Forecast Length

[32] The comparison of modeled and measured O_3 profiles strongly suggests that the modeled meridional stratospheric circulation in TM5—which is too fast—has large effects on modeled stratospheric O_3. This is consistent with findings in other studies as mentioned earlier. All previous

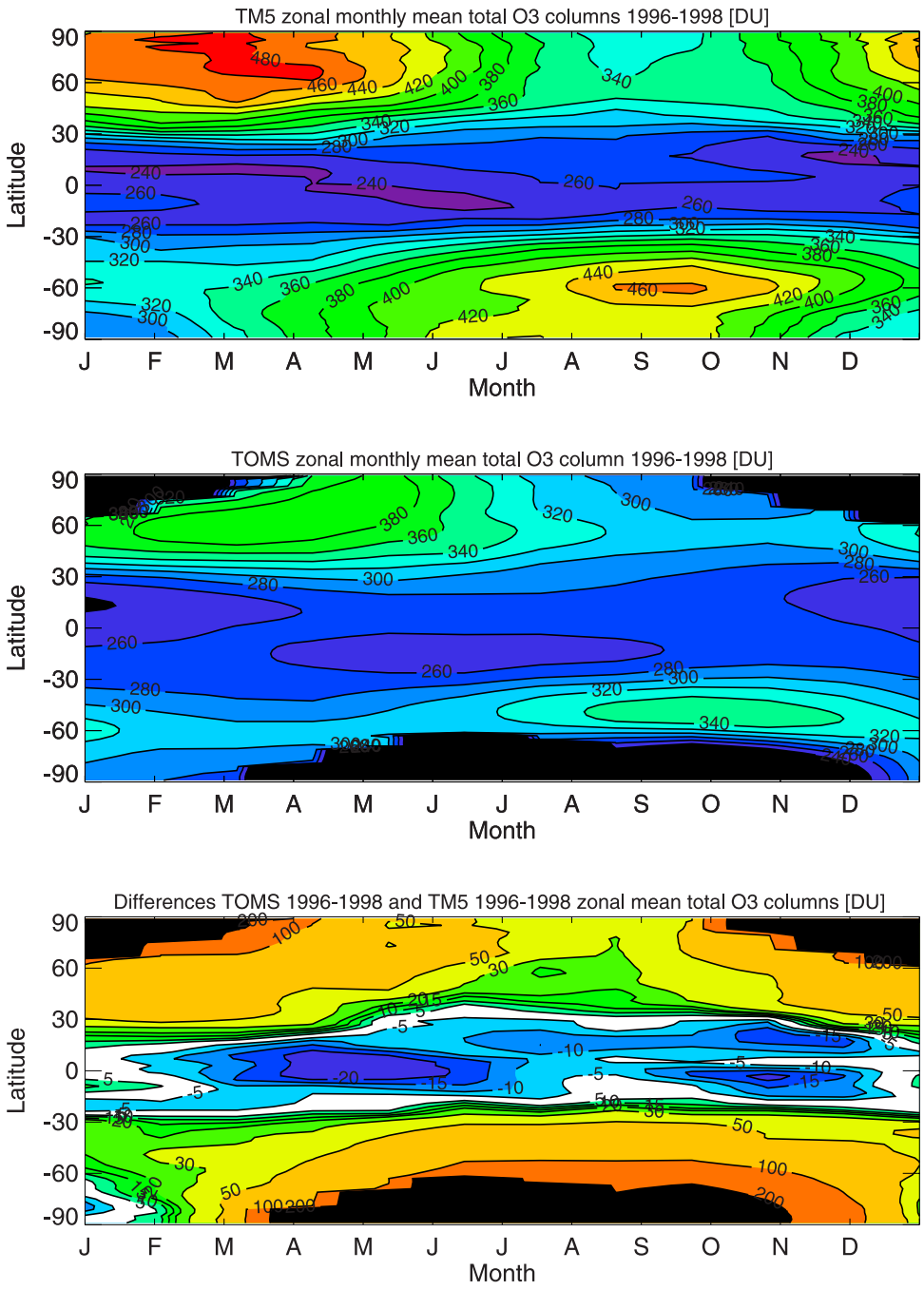

Figure 10. Comparison of seasonal variations in modeled (TM5) and measured (TOMS) zonal mean total O_3 columns for the period January 1996 to December 1998. Total O_3 column values are given in Dobson units (DU). The top plot shows the TM5 total O_3 columns, the middle plot shows the TOMS total O_3 columns, and the bottom plot shows the differences between TM5 and TOMS total O_3 columns. The black areas denote regions where no TOMS O_3 column measurements are available.

comparisons used ERA40 data derived from a 3DVAR data assimilation procedure. Here we explore model results based on winds from OD derived by more sophisticated 4DVAR data assimilation and which is expected to be less noisy. In addition, we explore the effect of increasing the forecast length which should improve the physical balance of the ECMWF winds. Figure 11a shows the comparison of sonde measurements and TM5 modeled O_3 with ERA40 and OD for the period January 2000 to December 2001. Note that these OD data consist of 6/12-hourly forecasts. Model results are compared with O_3 sonde measurements from Payerne, Switzerland, which should be representative for a typical midlatitude stratospheric station. A considerable difference reduction up to 50% appears in the lower extratropical stratosphere using OD compared to the model results using ERA40. Furthermore, the upper tropospheric/lower stratospheric vertical O_3 gradient is much more similar to what is measured.

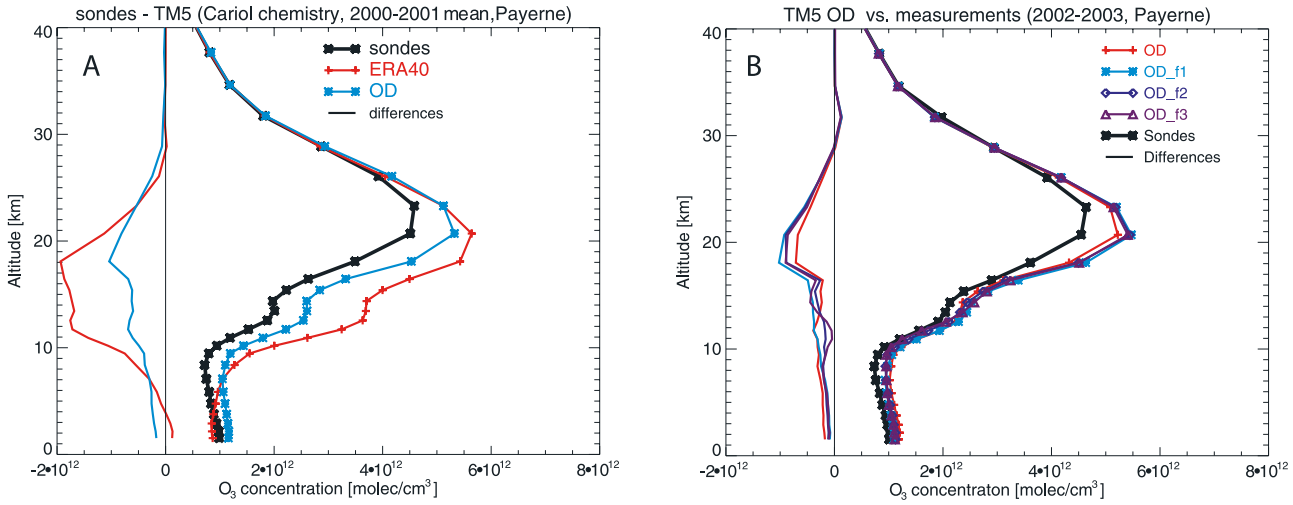

Figure 11. (a) Comparison between TM5 modeled and measured O_3 profiles for ERA40 data (red curve with pluses) and operational data with heterogeneous chemistry (blue curve with asterisks) for the period January 2000 to December 2001. TM5 results were collocated with O_3 sonde measurements (thick black curve with asterisks). Colored lines left of the zero line indicate the corresponding differences between the different TM5 simulations and sonde measurements. (b) Comparison between TM5 modeled and measured O_3 profiles for different OD forecasts: 6 hour forecast (red curve with pluses), 24 hour forecast (purple curve with triangles), 48 hour forecast (dark blue curve with squares), and 72 hour forecast (light blue curve with asterisks) for the period June 2002 to May 2003. The TM5 results were collocated with O_3 sonde measurements at Payerne. The colored lines left of the zero line indicate the corresponding differences between the different TM5 simulations and sonde measurements.

[33] Figures 12a and 12b show the zonal mean differences between the ERA40 and OD TM5 O3 simulations. Tropical stratospheric O_3 is higher whereas at midlatitude stratospheric O_3 is lower for the OD simulation as a result of a decreased transport from tropics to midlatitudes. At midlatitudes the vertical distribution of O_3 in the troposphere in the OD simulation shows less O_3 in the upper troposphere (less STE) and more O_3 (more UV radiation) near the surface. The reduction in STE also affects tropical tropospheric O_3 which is lower for the OD simulation. Some further improvement can be obtained by using different OD forecast lengths (24, 48 and 72 hour forecasts). Figures 13a, 13b, and 13c show the zonal mean differences between the different forecast periods simulations and the OD simulation. Consistent differences occur at higher latitudes in the upper troposphere/lowermost stratosphere and around the Northern Hemisphere subtropical jet. Largest differences are found for the simulation with the longest forecast period (3 days) but are much smaller than the ERA40-OD differences. Figure 11b shows that the effect is relatively small for Payerne and does not reduce the remaining stratospheric O_3 bias. These differences are consistent with the findings by *Meijer et al.* [2004] and *Scheele et al.* [2005], who obtained the best results with the longest forecast length, although the use of different OD forecast data appears to have a stronger effect on the age of air than on stratospheric O_3.

[34] Figure 14 shows a comparison between the TM5-OD simulation and sonde measurements for the period January 2000 to December 2001 for the same stations in Figure 6. Note that for station 1 (Sondankyla) and station 14 (Tateno) no O_3 sonde data were available for the period January 2000 to December 2001. At 25 km, the results differ only slightly from Figure 6. A small positive bias occurs at midlatitudes while a small negative bias occurs in the tropics. Results from a comparison at 25 km with an ERA40 reanalysis simulation for period January 2000 to December 2001 were similar to those in Figure 14 and thus different from those in Figure 6, reflecting the role of interannual variability (not shown). At 15 km, the differences between modeled and measured O_3 concentrations are much smaller compared to Figure 6, which is consistent with Figure 11. Note that now the model has a slight negative bias in the tropical lower stratosphere. Although the positive bias in the extratropical lower stratosphere decreases significantly by using OD data compared to ERA40, the bias does not completely disappear as a 20% bias remains at midlatitudes.

5. Summary and Discussion

[35] In this study GOME O_3 profiles were used for model evaluation, exploring the great advantage of improved spatial coverage and large number of spaceborne O_3 profile observations. We first compared the GOME and sonde measurements which showed a good agreement with differences on average less than 2% below 30 km and good (>0.8) time correlations for extratropical locations. Some of the differences may be related to GOME subpixel variability; the sonde and GOME measurements do not measure the exact same air masses. Furthermore, also clouds and aerosols affect O_3 profile retrievals and the sonde measurements have associated errors of up to 5% [*Harris et al.*, 1998]. A bias is present in tropical GOME O_3 measurements where they are systematically too high in the lower to middle stratosphere (up to 5×10^{11} molecules/cm^3

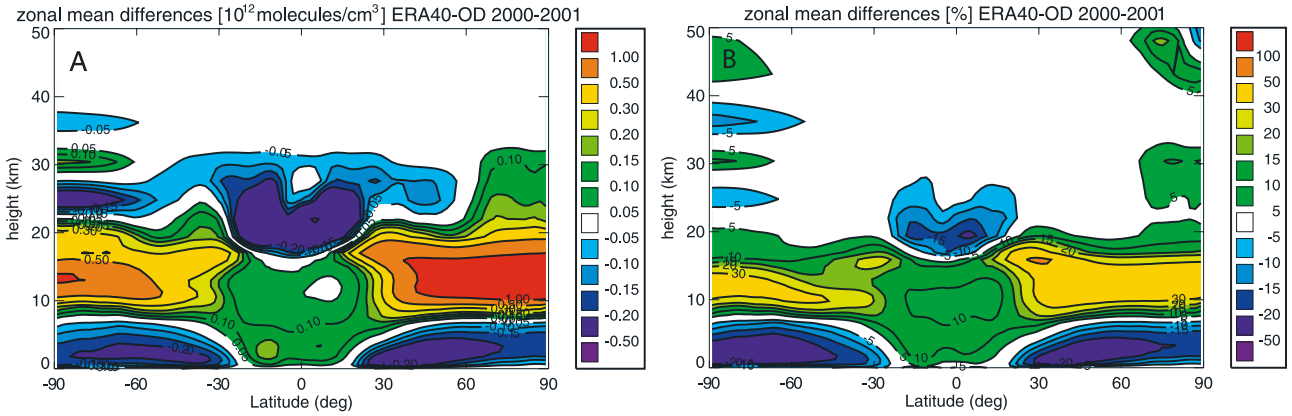

Figure 12. (a) Absolute (10^{12} molecules/cm^3) and (b) relative (%) zonal mean differences between the ERA40 and OD simulation for the period January 2000 to December 2001.

at 25 km) which is offset by too low O_3 in the troposphere and higher stratosphere.

[36] Next we explored possible causes of existing problems in stratospheric transport in CTMs when using DAS winds from NWP. We evaluated winds from different data assimilation procedures and different forecasts lengths in our model by extensive comparisons with GOME and sonde O_3 profiles. We used the TM5 model with linearized O_3 chemistry.

[37] Using DAS winds from 3DVAR assimilation (ERA40), the comparison between O_3 profile measurements (GOME, sonde) and TM5 showed that a systematic overestimation in the extratropical lower stratosphere and tropopause region exists in the TM5 modeled O_3 profiles. At 15 km, modeled O_3 concentrations are 40–50% too high, both for the sonde comparisons as well as for the GOME comparisons. This difference is found in both hemispheres, although only a few Southern Hemisphere O_3 sonde stations were available. At the same time a small negative stratospheric model bias was found in the tropics although a negative GOME bias in the tropical stratosphere complicates the interpretation of differences between TM5 results and measurements.

[38] The comparison between TOMS total O_3 columns and TM5 results are consistent with the findings from the GOME-TM5 comparison. Modeled and measured total O_3 columns are comparable at tropical latitudes, whereas the modeled total O_3 columns are too high at higher latitudes. The differences also have a strong seasonal signature, with the largest differences occurring in both hemispheres during local winter and the smallest differences occurring during local summer.

[39] These model biases and their particular height, latitude and seasonal dependence indicate that modeled stratospheric O_3 is affected by too fast meridional stratospheric transport due to the use of winds derived from the data assimilation system, as reported in previous studies [e.g., *Meijer et al.*, 2004; *Scheele et al.*, 2005]. It is important to note that a comparison between the O_3 climatology profiles from the linearized O_3 chemistry scheme and sonde measurements indicates that they agree very well in the stratosphere, so that the midlatitude model O_3 bias cannot be caused by the O_3 climatology in the linearized O_3 chemistry scheme. The linearized O_3 chemistry scheme certainly does have its limitations, especially for regions with fast O_3 chemistry like the upper stratosphere, as evidenced by *de Geer et al.* [2006], and the lower troposphere.

[40] The possibility that the differences found between observations and the TM5-ERA40 simulation are related to interannual variability is not very likely. The differences are significantly larger than observed stratospheric O_3 interannual variability; total column interannual variability does not exceed 10% [*World Meteorological Organization (WMO)*, 2002, pp. 4.8–4.15], although it should be noted that the limited periods for which TM5 simulations were performed (1996–1998, 2000–2001 and 2002) are not of

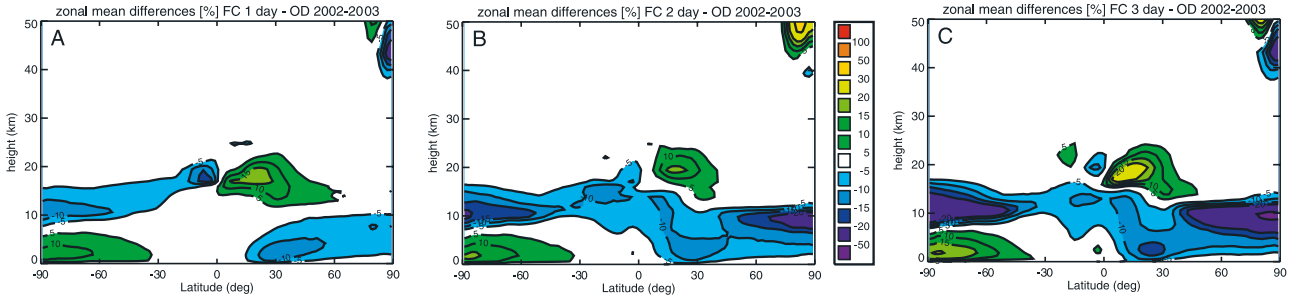

Figure 13. As in Figure 12b but for the differences between (a) 24 hour forecast, (b) 48 hour forecast, and (c) 72 hour forecast and the 6 hour OD forecasts for the period June 2002 to May 2003.

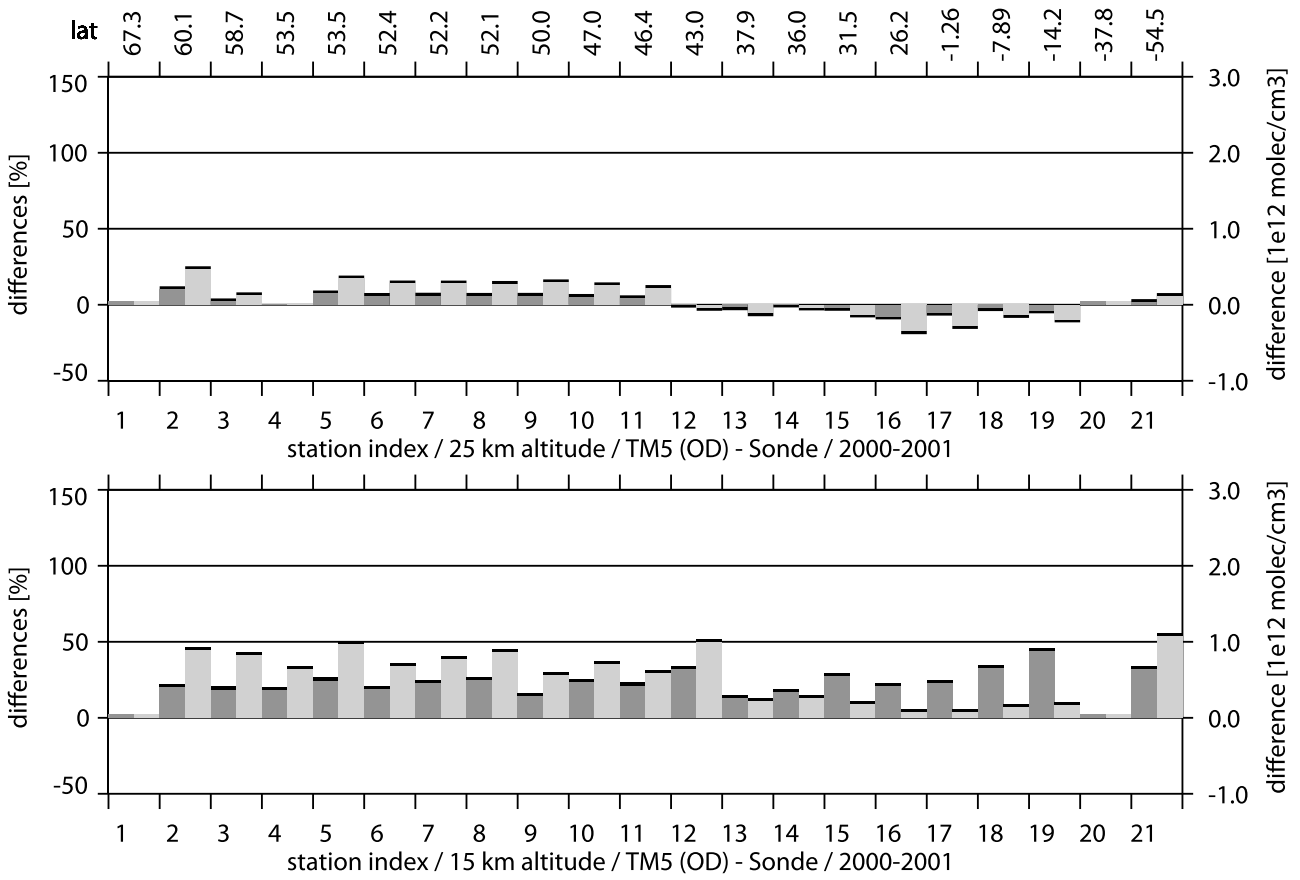

Figure 14. As in Figure 6 but for the TM5 simulation using OD data.

sufficient length to quantify the contribution of interannual variability to the differences.

[41] The explanation for the differences between the TM5-ERA40 simulations and measurements is that ERA40 is continuously perturbed by the assimilation of observations, and therefore cannot reach an internal physically consistent balance (meridional stratospheric transport is only a residual circulation due to the near-balanced zonal circulation and thus is very sensitive to small perturbations in the zonal balance). These findings are consistent with those reported by *Douglass et al.* [2003] that the assimilation of temperature and wind fields can act as an "additional forcing," which leads to unrealistic stratospheric transport.

[42] Using winds derived from more sophisticated 4DVAR data assimilation (OD) resulted in a large improvement at 15 km in the extratropics: differences are reduced from about 40–50% to 15–30% at midlatitudes. This reveals that a 4DVAR assimilation procedure reduces the noise and results in more physically balanced wind fields which affects the stratospheric meridional transport and consequently downward transport into the troposphere.

[43] Some uncertainty in our comparison is introduced by the lack of heterogeneous chemistry in the model. Studies of stratospheric O_3 measurements found on average a reduction of stratospheric O_3 by several percents over the period 1980–2000 [*WMO*, 2002]. For a given year the reduction can be larger (up to 10%). However, the model bias using OD winds was 15–30% and is thus too large to be fully explained by heterogeneous photochemical O_3 destruction. Furthermore, results from *Hadjinicolaou and Pyle* [2004] indicate that this O_3 loss predominantly occurs at polar latitudes during the winter season. The bias is present throughout the year, which is an additional indication that other processes than polar stratospheric O_3 loss must be causing differences.

[44] We also explored increased forecast length of 1, 2 and 3 days, respectively, which mainly affect high-latitude lower stratospheric O_3 with the largest differences occurring for the longest forecast length. The use of different forecast lengths appears to have a larger effect on the age of air [*Meijer et al.*, 2004; *Scheele et al.*, 2005] than on stratospheric O_3. This might be related to the different stratospheric chemistry of O_3 and the long-lived tracers used for age-of-air calculations and is an important topic for future research.

[45] It is remarkable that, at 25 km, OD results in too high O_3, in contrast to the results from ERA40 (compare Figures 6 and 13). In addition, the evaluation of OD shows considerable differences between 2000 and 2002, possibly indicating interannual variability of the model performances. Ideally, the detailed evaluation presented here should be performed for every year for which sufficient data are available. This is beyond the scope of this work, but an interesting issue for future studies. Future work should also involve the evaluation of time discretization of the DAS winds, for example 3-hourly versus 6-hourly winds and other data assimilation procedures [*Polavarapu et al.*, 2005; *Bregman et al.*, 2006].

[46] **Acknowledgments.** The authors thank the referees for their suggestions in helping improve this paper.

References

Braesicke, P., and J. A. Pyle (2003), Changing ozone and changing circulation in northern mid-latitudes: Possible feedback?, *Geophys. Res. Lett.*, *30*(2), 1059, doi:10.1029/2002GL015973.

Brasseur, G. P., J. J. Orlando, and G. S. Tyndall (1999), *Atmospheric Chemistry and Global Change*, 502 pp., Oxford Univ. Press, New York.

Bregman, A., M. C. Krol, J. Teyssedre, W. A. Norton, A. Iwi, M. Chipperfield, G. Pitari, J. K. Sundet, and J. Lelieveld (2001), Chemistry-transport model comparison with ozone observations in the midlatitude lowermost stratosphere, *J. Geophys. Res.*, *106*, 17,479–17,496.

Bregman, A., A. Segers, M. Krol, E. Meijer, and P. van Velthoven (2003), On the use of mass-conserving wind fields in chemistry-transport models, *Atmos. Chem. Phys.*, *3*, 447–457.

Bregman, A., E. Meijer, and R. Scheele (2006), Key aspects of stratospheric tracer modeling, *Atmos. Chem. Phys. Discuss.*, *6*, 4375–4414.

Brewer, A. W. (1949), Evidence for a world circulation provided by the measurements of helium and water vapor distribution in the stratosphere, *Q. J. R. Meteorol. Soc.*, *75*, 351–363.

Cariolle, D., and M. Déqué (1986), Southern Hemisphere medium-scale waves and total ozone disturbances in a spectral general circulation model, *J. Geophys. Res.*, *91*, 10,825–10,846.

de Geer, A. J., et al. (2006), The ASSET intercomparison of ozone analyses: Method and first results, *Atmos. Chem. Phys. Discuss.*, *6*, 4495–4577.

Dessler, A. (2000), *The Chemistry and Physics of Stratospheric Ozone*, *Int. Geophys. Ser.*, vol. 74, pp. 117–136, Elsevier, New York.

Dobber, M. R., A. P. H. Goede, and J. Burrows (1998), Observations of the moon by the global ozone monitoring experiment: Radiometric calibration and lunar albedo, *Appl. Opt.*, *37*, 7832–7841.

Dobson, G. M. B. (1956), Origin and distribution of polyatomic molecules in the atmosphere, *Proc. R. Soc. London, Ser. A*, *236*, 187–193.

Douglass, A. R., M. R. Schoeberl, R. B. Rood, and S. Pawson (2003), Evaluation of transport in the lower tropical stratosphere in a global chemistry and transport model, *J. Geophys. Res.*, *108*(D9), 4259, doi:10.1029/2002JD002696.

Fortuin, J. P. F., and H. Kelder (1998), An ozone climatology based on ozonesonde and satellite measurements, *J. Geophys. Res.*, *103*(D24), 31,709–31,734.

Hadjinicolaou, P., and J. A. Pyle (2004), The impact of arctic ozone depletion on northern middle latitudes: Interannual variability and dynamical control, *J. Atmos. Chem.*, *47*, 25–43.

Hadjinicolaou, P., J. A. Pyle, and N. R. P. Harris (2005), The recent turnaround in stratospheric ozone over northern middle latitudes: A dynamical modeling perspective, *Geophys. Res. Lett.*, *32*, L12821, doi:10.1029/2005GL022476.

Harris, R., R. Hudson, and C. Phillips (1998), Assessment of trends in the vertical distribution of ozone, *SPARC Rep. 1*, *WMO Proj. Rep. 43*, World. Meteorol. Org., Ozone Res. Monit. Proj., Geneva, Switzerland.

Hasekamp, O. P., and J. Landgraf (2001), Ozone profile retrieval from backscattered ultraviolet radiances: The inverse problem solved by regularization, *J. Geophys. Res.*, *106*, 8077–8088.

Hasekamp, O. P., J. Landgraf, and R. van Oss (2002), The need of polarization modeling for ozone profile retrieval from backscattered sunlight, *J. Geophys. Res.*, *107*(D23), 4692, doi:10.1029/2002JD002387.

Hoogen, R., V. V. Rozanov, and J. P. Burrows (1999), Ozone profiles from GOME satellite data: Algorithm description and first validation, *J. Geophys. Res.*, *104*, 8263–8280.

Joeckel, P., R. von Kuhlmann, M. G. Lawrence, B. Steil, C. A. M. Brenninkmeijer, P. J. Crutzen, P. J. Rasch, and B. Eaton (2001), On a fundamental problem in implementing flux-form advection schemes for tracer transport in 3-dimensional general circulation and chemistry transport models, *Q. J. R. Meteorol. Soc.*, *127*, 1035–1052.

Krol, M. C., S. Houweling, A. Bregman, M. M. P. van den Broek, A. J. Segers, P. F. J. van Velthoven, W. Peters, F. J. Dentener, and P. Bergamaschi (2005), The two-way nested global chemistry-transport zoom model TM5: Algorithm and applications, *Atmos. Chem. Phys.*, *5*, 417–432.

Landgraf, J., and O. P. Hasekamp (2002), Ozone profile retrieval from satellite measurements of nadir backscattered light in the ultraviolet of the solar spectrum, *Recent Res. Dev. Geophys.*, *4*, 157–189.

Liu, X., K. Chance, C. E. Sioris, R. J. D. Spurr, T. P. Kurosu, R. V. Martin, and M. J. Newchurch (2005), Ozone profile and tropospheric ozone retrievals from the Global Ozone Monitoring Experiment: Algorithm description and validation, *J. Geophys. Res.*, *110*, D20307, doi:10.1029/2005JD006240.

McCormack, J. P., et al. (2004), NOGAPS-ALPHA model simulations of stratospheric ozone during the SOLVE2 campaign, *Atmos. Chem. Phys.*, *4*, 2401–2423.

McLinden, C. A., S. C. Olsen, B. Hannegan, O. Wild, M. J. Prather, and J. Sundet (2000), Stratospheric ozone in 3-D models: A simple chemistry and the cross-tropopause flux, *J. Geophys. Res.*, *105*, 14,653–14,665.

McPeters, R. D., et al. (1996), Nimbus-7 Total Ozone Mapping Spectrometer (TOMS) data products user's guide, *NASA Ref. Publ.1384*, NASA, Silver Spring, Md.

Meijer, E. W., B. Bregman, A. Segers, and P. F. J. van Velthoven (2004), The influence of data assimilation on the age of air calculated with a global chemistry-transport model using ECMWF wind fields, *Geophys. Res. Lett.*, *31*, L23114, doi:10.1029/2004GL021158.

Olsen, M. A., M. R. Schoeberl, and A. R. Douglass (2004), Stratosphere-troposphere exchange of mass and ozone, *J. Geophys. Res.*, *109*, D24114, doi:10.1029/2004JD005186.

Polavarapu, S., S. Z. Ren, Y. Rochon, D. Sankey, N. Ek, J. Koshyk, and D. Tarasick (2005), Data assimilation with the Canadian middle atmosphere model, *Atmos. Ocean*, *43*, 77–100.

Rodgers, C. D. (1990), Characterization and error analysis of profiles retrieved from remote sounding measurements, *J. Geophys. Res.*, *95*, 5587–5595.

Rood, R. B., A. R. Douglass, M. C. Cerniglia, L. C. Sparling, and J. E. Nielsen (2000), Seasonal variability of middle-latitude ozone in the lowermost stratosphere derived from probability distribution functions, *J. Geophys. Res.*, *105*, 17,793–17,805.

Scheele, M. P., P. C. Siegmund, and P. F. J. van Velthoven (2005), Stratospheric age of air computed with trajectories based on various 3D-Var and 4D-Var data sets, *Atmos. Chem. Phys.*, *5*, 1–7.

Schoeberl, M. R., A. R. Douglass, Z. Zhu, and S. Pawson (2003), A comparison of the lower stratospheric age spectra derived from a general circulation model and two data assimilation systems, *J. Geophys. Res.*, *108*(D13), 4113, doi:10.1029/2002JD002652.

Segers, A., P. van Velthoven, A. Bregman, and M. Krol (2002), On the computation of mass fluxes for Eulerian transport models from spectral meteorological fields, in *Proceedings of the 2002 International Conference on Computational Science, Lecture Notes in Computer Science (LNCS)*, edited by E. Ong et al., pp. 767–776, Springer, New York.

Segers, A. J., H. J. Eskes, R. J. van der A, R. F. van Oss, and P. F. J. van Velthoven (2005), Assimilation of GOME ozone profiles and a global chemistry-transport model using a Kalman filter with anisotropic covariance, *Q. J. R. Meteorol. Soc.*, *131*, 477–502.

Strahan, S. E., and A. R. Douglass (2004), Evaluating the credibility of transport processes in simulations of ozone recovery using the Global Modeling Initiative three-dimensional model, *J. Geophys. Res.*, *109*, D05110, doi:10.1029/2003JD004238.

van den Broek, M. M. P., M. K. van Aalst, A. Bregman, M. Krol, J. Lelieveld, G. C. Toon, S. Garcelon, G. M. Hansford, R. L. Jones, and T. D. Gardiner (2003), The impact of model grid zooming on tracer transport in the 1999–2000 Arctic polar vortex, *Atmos. Chem. Phys.*, *3*, 1833–1847.

van den Broek, M. M. P., J. E. Williams, and A. Bregman (2004), Implementing growth and sedimentation of NAT particles in a global Eulerian model, *Atmos. Chem. Phys.*, *4*, 1869–1883.

van der A, R. J., R. F. van Oss, A. J. M. Piters, J. P. F. Fortuin, Y. J. Meijer, and H. M. Kelder (2002), Ozone profile retrieval from recalibrated Global Ozone Monitoring Experiment data, *J. Geophys. Res.*, *107*(D15), 4239, doi:10.1029/2001JD000696.

Waugh, D., and T. Hall (2002), Age of stratospheric air: Theory, observations, and models, *Rev. Geophys.*, *40*(4), 1010, doi:10.1029/2000RG000101.

World Meteorological Organization (2002), Scientific assessment of ozone depletion: 2000, *WMO Proj. Rep. 47, Executive Summary*, pp. 9, World Meteorol. Org., Global Ozone Res. Monit. Proj., Geneva, Switzerland.

I. Aben, O. Hasekamp, and J. Landgraf, Netherlands Institute for Space Research, Sorbonnelaan 2, NL-3584 CA, Utrecht, Netherlands.

B. Bregman, TNO Built Environment and Geosciences, NL-7300 AH, Apeldoorn, Netherlands.

A. T. J. de Laat, Royal Netherlands Meteorological Institute, NL-3732 GK De Bilt, Netherlands. (jos.de.laat@knmi.nl)